FUSION RESEARCH CENTER

DOE/ER/54241--144

DOE/ER/542-41-144 FRCR #463

The dynamics of core temperature fluctuations during sawtooth oscillations on TEXT-U

Christopher Watts
R. F. Gandy

Department of Physics
Auburn University
Auburn, AL 36849

May 3, 1995

THE UNIVERSITY OF TEXAS

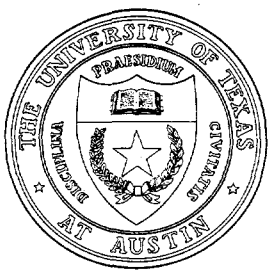

Austin, Texas

DISCLAIMER

The dynamics of core electron temperature fluctuations during sawtooth oscillations on TEXT-U.

Christopher Watts, R. F. Gandy
Department of Physics, Auburn University, Auburn, AL 36849

52.25.Fi, 52.25.Gj, 52.70.Gw, 52.55.Fa

Core electron temperature fluctuations are measured in a tokamak plasma where some degree of time resolution is achieved. There is a strong correlation between the turbulence level and the phase of the sawtooth oscillation. A global linear relationship between the temperature fluctuation amplitude and the electron temperature gradient scale length is found. The enhancement in fluctuations at the sawtooth crash is correlated to a steepening of the electron temperature gradient created as the sawtooth heat pulse propagates outward.

Toroidal, magnetic confinement schemes still suffer from anomalously poor confinement and, as yet, the mechanism causing this transport is poorly understood. Turbulent electrostatic fluctuations are considered by many as one likely candidate responsible for the transport [1-4]. This fluctuation-induced transport consists of two components, a particle flux Γ_e, and a heat flux Q_e, given by

$$\Gamma_e = \langle \tilde{n}_e \tilde{v}_e \rangle = \langle \tilde{n}_e \tilde{E}_\theta \rangle / B \tag{1}$$

$$Q_e = \frac{3}{2}\langle \tilde{p}_e \tilde{v}_e \rangle = \frac{3}{2} n_e \langle \tilde{T}_e \tilde{E}_\theta \rangle / B + \frac{3}{2} T_e \Gamma_e \tag{2}$$

Here, $\tilde{n}_e$, $\tilde{T}_e$ and $\tilde{p}_e$ represent the fluctuations in electron density, temperature and pressure, and $\tilde{v}_e \approx \tilde{E}_\theta / B = -\nabla_\theta \tilde{\varphi} / B$ is the radial component of the fluctuating $\mathbf{E} \times \mathbf{B}$ velocity. Thus the particle flux component results from the correlated fluctuations of plasma electric field and electron density, while the conducted heat flux is due to correlated fluctuations of the electric field and electron temperature.

Very recently, electron temperature fluctuations, $\tilde{T}_{e,\mathrm{rms}} / T_e$, have been measured in both stellarator [5] and

tokamak [6-8] plasmas using a technique correlating the plasma electron cyclotron emission (ECE). On TEXT-U correlation radiometry of ECE (CRECE) correlates the emission of two largely overlapping sample volumes in two disjoint frequency bands [6-8]. This eliminates the random, uncorrelated inherent wave noise of the ECE signal while retaining the common temperature fluctuation amplitude. Detailed power spectra of these temperature fluctuations have been obtained over the low field side of the plasma in the equatorial plane [6]. Unfortunately, in order to reduce the wave noise to an acceptable level requires long time averaging, on the order of one second, and any temporal information of the turbulent fluctuations is lost.

In this letter we report results in which some temporal information has been distilled. The quasi-periodic nature of tokamak sawtooth oscillations allows one to perform the correlation analysis synchronously with these oscillations, and thereby obtain spectra representing the evolution of the temperature fluctuations during the course of an average sawtooth period. (Sawteeth are characterized by a sudden drop (~5-10%) in the electron temperature of the plasma core, followed by a rise in temperature outside the sawtooth inversion radius.) This provides some understanding of the time evolution of the temperature fluctuations, and perhaps insight into the mechanism of electrostatic turbulence and associated transport. The tacit assumption is that the dynamics of the turbulence are reproducibly linked to the sawtooth oscillations, a hypothesis verified *a posteriori.*

Measurements reported here have been made as outlined in [6] for circular plasmas (R=105 cm, a=27 cm) with B_ϕ=~2 T, I_p=200 kA and $\bar{n}_e$= 2x10^{13}cm^{-3}. Measurements are made in the equatorial plane from the low field side. The sample volume is a disk approximately 2 cm in diameter and 0.8 cm thick in the radial direction, allowing detection of wavenumbers $k_\theta \lesssim 2$ cm^{-1} and $k_r \lesssim 5$ cm^{-1}. Figure 1 shows the electron temperature profile(s) typical of these discharges, one during the quiescent period between sawtooth crashes (gray) and the second during the sawtooth crash (black). A QuickTime movie of the evolution of the temperature profile during a sawtooth oscillation is available on the Fusion Research Center gopher server†. The plots were made by sweeping the plasma horizontally ±1.5 cm during a single TEXT-U discharge, and a set of 8 fixed ECE

---

† The movie, created by G. Cima, is available from the gopher server hagar.ph.utexas.edu in the directory TEXT-U Tokamak Information/TEXT-U Data and Experiments/ECE QuickTime Movie.

channels recorded the electron temperature. This was used to reconstruct the profile by matching the temperature in the overlapping region of two adjacent channels. The sawtooth inversion radius is located at $r/a \approx 0.35$ for these discharges.

To obtain the evolution of the temperature fluctuations during a sawtooth oscillation, ECE data are subdivided into eight bins representing different phases of the oscillation. All phases are relative to the *local* sawtooth crash at the measurement location. The data in each phase are Fourier analyzed with a frequency resolution of 1/32 of the Nyquist frequency to produce the time-averaged power spectrum for each sawtooth phase. Successive sawteeth are treated similarly, and the spectra of each sawtooth phase are ensemble averaged over many sawteeth to obtain the requisite statistics; each spectrum incorporates about 1000 sawteeth representing a 200 ms time average. A typical sawtooth oscillation has a period of about 1.5 ms. However, because sawteeth periods are irregular, the number of points in each phase bin will vary. In addition, there is some ambiguity in determining the exact time of the sawtooth crash; the error is about ± 50 μs.

Figure 2 depicts the evolution of the temperature fluctuation spectrum at $r/a=0.13$, which is well inside the sawtooth inversion radius. Plotted is the normalized fluctuation power for each of the eight phases of a sawtooth oscillation (black line) along with the sawtooth averaged spectrum (gray), which is the same in each plot. The phases are labeled A-H, with A occurring at the sawtooth crash; the convention is sketched in the inset figure of plot A. The dashed horizontal line represents the limit of statistical significance; points above this level are significant with regards to the correlation technique used to extract the temperature fluctuation from the inherently noisy ECE signal (see [6]). The spectra are normalized to the average electron temperature level for that particular sawtooth phase. Hence, changes in the spectra represent only changes in the relative fluctuation level independent of any change in the bulk electron temperature.

As reported elsewhere [7], in the core ($r/a \approx 0$) before and during the sawtooth crash (phases H and A) there is a dramatic rise, on the order of a factor of ten, in the turbulence level at low frequency (<50 kHz). Ambiguity in determining the exact crash time distributes the energy between the two phase bins that straddle the crash, A and H; the increase in fluctuation energy can be localized to a window of about 200 μs around the peak of the sawtooth crash. Analysis of soft x-ray data, numerical and analytical models indicates that this energy increase

is attributable to the Fourier components of the sudden temperature drop in signal at the sawtooth crash (the power spectrum of the sawtoothing signal). After the crash, no significant turbulence is seen above the statistical limit except at very low frequencies (<25 kHz). Because of the relatively small signal, phases C through G have been ensemble averaged in order to obtain reasonable statistics. (The statistical noise level is less than 10^{-10} for this plot.) Figure 3 clarifies the trend by plotting the electron temperature fluctuation amplitude, $\tilde{T}_{e,\mathrm{rms}} / \bar{T}_e$, integrated over frequencies above 25 kHz. (Integration yields sufficient statistics, and phases C-G need no longer be averaged.) The lower frequency limit is chosen to eliminate low-frequency MHD oscillations.

Figure 4 show the evolution at *r/a*=0.54, outside the sawtooth inversion radius. Looking first at the sawtooth averaged spectrum (gray line), immediately apparent is the appearance of a second "feature" in the spectrum which peaks at about 150 kHz. This "bump" is localized to the gradient region of the temperature profile, and is distinguishable at all radii outside the inversion radius surface [6, 7]. The center of the bump moves to lower frequency as one moves radially outward. Assuming a plasma $E\mathrm{x}B$ rotation velocity as measured by the heavy ion beam probe (HIBP) [9], the bump is consistent with a Doppler shifted turbulence feature rotating with the electron diamagnetic drift velocity, $\omega_e^* = k_\theta T_e / eB\alpha_n$. α_n is the density gradient scale length. Density fluctuation diagnostics identify a similar feature in their spectra and find that this mode propagates in the electron diamagnetic drift direction [9, 10].

As in the core, during the sawtooth crash the fluctuation level increases dramatically (phase A). This increase, however, is not confined exclusively to low frequency, but extends over the entire spectrum, and hence cannot be explained by the Fourier components of the sawtoothing signal. Immediately after the crash the fluctuation power drops over the entire spectrum and continues to drop until about phase C (figure 3) when the energy seems to be largely dissipated. For the reasons cited above, phases D-H have been ensemble averaged. The fluctuations remain at this low level for the remainder of the sawtooth period.

A plausible mechanism for the observed energy loss would be a net propagation outward. However, data presented in [11] and [7] belie this scenario. We find non-zero cross-coherence, but zero cross-phase at all frequencies for sample volumes separated radially by up to 3 cm. This implies a mean radial wavenumber $\bar{k}_r = 0$, indicating that there is no net radial propagation of these temperature fluctuations. The results imply that

the energy is lost via some diffusive process, where a plausible mechanism is that the energy is dissipated at high k modes [4, 12].

Figure 3 also shows data taken at *r/a*=0.65. As before, there is an enhancement in the fluctuation energy at the crash which relaxes over the course of the sawtooth period. However, the effect is not as dramatic as at *r/a*=0.54, and the enhancement lasts over several sawtooth phases (A-D). This indicates that the energy source enhancing the turbulence is weaker, albeit more long lived. Further, only part of the energy has dissipated by the final two phases. It appears that either the dissipation mechanism is not as efficient, or the steady-state (between sawtooth crash) driving mechanism is stronger. Farther out in radius the effect of sawteeth on the spectra is minimal.

In order to understand the turbulence enhancement we look again to the evolution of the electron temperature profile during a sawtooth oscillation shown in figure 1. Concentrating first on the quiescent profile, there are two prominent regions: the flat region of the profile inside the sawtooth inversion radius, and the gradient region outside. It is in the gradient region where the "bump" in the power spectra appears; inside the inversion radius all power is confined to low frequency. The implication is that the gradient, which is widely theorized to be the energy source of electron turbulence [1, 2, 12], .is indeed source for the turbulent fluctuations in "bump" region.

During a sawtooth crash, inside the inversion radius (the flat region) the entire profile rises and collapses simultaneously resulting in only a small change in the electron temperature gradient. Coincident with this there is a rise in only the low frequency (<~70 kHz) turbulent temperature fluctuations which is associated with the discontinuous nature of the crash. Outside the inversion radius, however, the propagating heat pulse leads to a significant steepening of the gradient. One sees a commensurate enhancement of the temperature fluctuations in the "bump" region of the spectra. This increase in gradient the likely source of the energy enhancing the turbulence further out in radius. At mid radius the change in gradient is significant as the heat pulse propagates outward, and there is a large rise in the turbulence level. Farther out in radius the heat pulse is less potent, resulting in a smaller gradient change over a longer time period. This would account for the smaller increase in the turbulence level and longer duration of the enhancement observed at larger radii.

To quantify this effect in figure 5 is plotted the temperature fluctuation amplitude, $\tilde{T}_{e,\mathrm{rms}} / T_e$, integrated over

the bump region (75-225 kHz) versus the electron temperature gradient scale length $\alpha_T = |T_e/(dT_e/dr)|$, normalized to the plasma minor radius. Each of the 8 points at each radii represent the eight phases of the sawtooth oscillation. Immediately apparent is the global linear relationship between fluctuation amplitude and α_T, reflecting the fact that the fluctuations increase with increasing radius. More significant, however, is that during the crash phase (hollow symbols) α_T decreases while the fluctuations increase. Thus, as the sawtooth heat pulse propagates outward there is a steepening of the temperature gradient and a commensurate rise in the temperature fluctuation amplitude. However, it is not clear that change in fluctuation amplitude is consistent with the global linear relationship. The data indicate, rather, that the temperature fluctuations increase significantly for only modest changes in α_T. The global linear scaling of $\tilde{T}_{e,\mathrm{rms}}/T_e$ vs. α_T appears to contradict marginal stability theories of anomalous transport, which argue that small changes in the temperature profile should result in a tremendous increase in fluctuation amplitude to re-stabilize the profile [1]. However, data during the sawtooth heat pulse appear to be consistent with marginal stability theories, since the temperature fluctuations rise dramatically for modest changes in the local temperature gradient. More detailed profiles of both the temperature fluctuations and the temperature gradient scale length are needed before a definitive conclusion is possible.

The significance of these results with regards to electrostatic transport has yet to be determined. Data are not yet available from the HIBP to ascertain whether a similar evolution of plasma potential fluctuations occurs. Further, since the wavenumber spectrum of these temperature fluctuations is difficult to measure, the relevance of the fluctuations in eq. (2) is uncertain. One would expect, however, that any effect of the sawteeth on transport is predominantly local, and likely does not effect observed global anomalous transport significantly; the turbulence enhancement, which is large only for $r/a<0.6$, represents a small perturbation when integrated over both plasma radius and time.

Transport studies of sawtooth-free discharges are ambiguous. Results from ASDEX indicate an enhancement of confinement, though this is likely due to effects other than simply the lack of sawteeth (see [13] and references therein), while results from JET indicate no change in confinement when comparing discharges with "normal" and "monster" (ultra-long period) sawteeth [14]. In the edge a similar correlation between sawtooth oscillations and turbulent fluctuations has been identified, the sawtooth crash resulting in a significant increase in the associated

transport [15]. Results from experiments modifying the equilibrium density and temperature profiles indicate that ∇T_e does not effect electrostatic particle flux, but draws no conclusions as to electrostatic heat flux.

We plan to explore these issues more fully in future work to concentrate in the following areas: Potential measurements will be made using the HIBP to ascertain whether the potential fluctuations evolve similarly to temperature fluctuations during a sawtooth oscillation. Work is in progress to better determine the spatial resolution of the CRECE system and hence better determine the wavenumber spectrum of the turbulence. Measurements are being made of the plasma top and high field side to determine whether these fluctuations show any poloidal asymmetry, indicative of trapped particle modes. Finally, recent experiments have demonstrated that sawtooth oscillations can be enhanced or suppressed with electron cyclotron heating and proper beam orientation. Thus the effect of sawtooth amplitude on the turbulence level can be studied.

In summary, by using the quasi-periodic nature of tokamak sawtooth oscillations we have obtained some temporal resolution of the turbulent electron temperature fluctuations. Analysis of the data shows that the fluctuation level is intimately linked to the phase of the sawtooth oscillation, and a strong enhancement of fluctuations power is seen at the sawtooth crash. A "bump" feature is seen in the power spectra outside the sawtooth inversion radius which is enhanced during the sawtooth crash. We identify this bump as being due to the electron temperature gradient, and the enhancement during the crash is due to the steepening of the gradient as the sawtooth heat pulse propagates outward. We find a global linear relationship between $\tilde{T}_{e,\mathrm{rms}} / T_e$ in the bump region and the temperature gradient scale length. However, during a sawtooth oscillation the enhancement of the temperature fluctuations is greater than the scaling law predicets for the change in the local gradient scale length. Further study is needed to assess the relevance of these finding to anomalous transport.

We would like to thank David E. Newman, Pepi Cima, Alan Wootton and Ken Gentle for their significant contribution in the form of discussions. This work is supported by the United States Department of Energy under grants DE-FG05-90ER54085-95 and DE-FG03-94ER-54241.

References

1 P. C. Liewer, Nucl. Fusion, **25**, 543 (1985).

2 F. Wagner and U. Stroth, Plasma Phys. Controlled Fusion, **35**, 1321 (1993).

3 J. Sheffield, Rev. Mod. Phys., **66**, 1015 (1994).

4 D. E. Newman, P. W. Terry, P. H. Diamond, Y. Liang, G. G. Craddock, A. E. Koniges and J. A. Crotinger, Phys. Plasmas, **1**, 1592 (1994).

5 S. Sattler, H. J. Hartfuss and W.-A. Team, Phys. Rev. Lett., **72**, 653 (1994).

6 G. Cima, T. D. Rempel, R. V. Bravenec, R. F. Gandy, M. Kwon, C. Watts and A. J. Wootton, Phys. Plasmas, **2** (1995).

7 C. Watts, G. Cima, R. F. Gandy and T. D. Rempel, Rev. Sci. Instrum., **66**, 451 (1995).

8 G. Cima and C. Watts, Rev. Sci. Instrum., **66**, 798 (1995).

9 A. Fujisawa, A. Ouroua, J. W. Heard, T. P. Crowley, P. M. Schoch, K. A. Conner, R. L. Hickok and A. J. Wootton, *submitted to* Physical Review Letters (1995).

10 Y. Karzhavin, *personal communicaion.*

11 C. Watts, G. Cima and R. F. Gandy, in *Proceedings of EC-9, The 9th Joint Workshop on Electron Cyclotron Emission and Electron Cyclotron Resonance Heating,* Borrego Springs, CA (1995).

12 D. E. Newman, P. W. Terry and P. H. Diamond, Phys. Fluids B, **4**, 599 (1992).

13 U. Stroth, G. Fussmann, K. Krieger, V. Mertens, F. Wagner, M. Bessenrodt-Weberpals, R. Büchse, L. Giannone, W. Herrmann, E. Simmet, K. Steuer and A. Team, Nucl. Fusion, **31**, 2291 (1991).

14 V. P. Bhatnagar, D. Campbell, J. P. Christiansen, J. G. Cordey, J. Jacquinot, D. F. H. Start, P. Thomas and K. Thomsen, in *Proceedings from the 15th European Conference on Controlled Fusion and Plasma Heating,* S. Pešic′ and J. Jacquinots, eds., Dubrovnik, Yugoslavia (European Physical Society, 1988) vol. 12, part I, 358.

15 T. L. Rhodes, C. P. Ritz and H. Lin, Phys. Rev. Lett., **65**, 583 (1990).

Figure Captions

Figure 1. Electron temperature profile about mid-way between sawtooth crashes (gray line), and during a crash (black). The profile steepens significantly outside the sawtooth inversion radius (flat region) during the sawtooth.

Figure 2. Evolution of the electron temperature fluctuation power spectrum during a sawtooth oscillation at r/a=0.13 (black). The gray line is the same spectrum averaged over sawteeth.

Figure 3. Integrated electron temperature fluctuation amplitude for each of the sawtooth phases.

Figure 4. Evolution of the electron temperature fluctuation power spectrum at r/a=0.54.

Figure 5. Temperature fluctuation amplitude in the bump region vs. temperature gradient scale length. Error bars are representative.

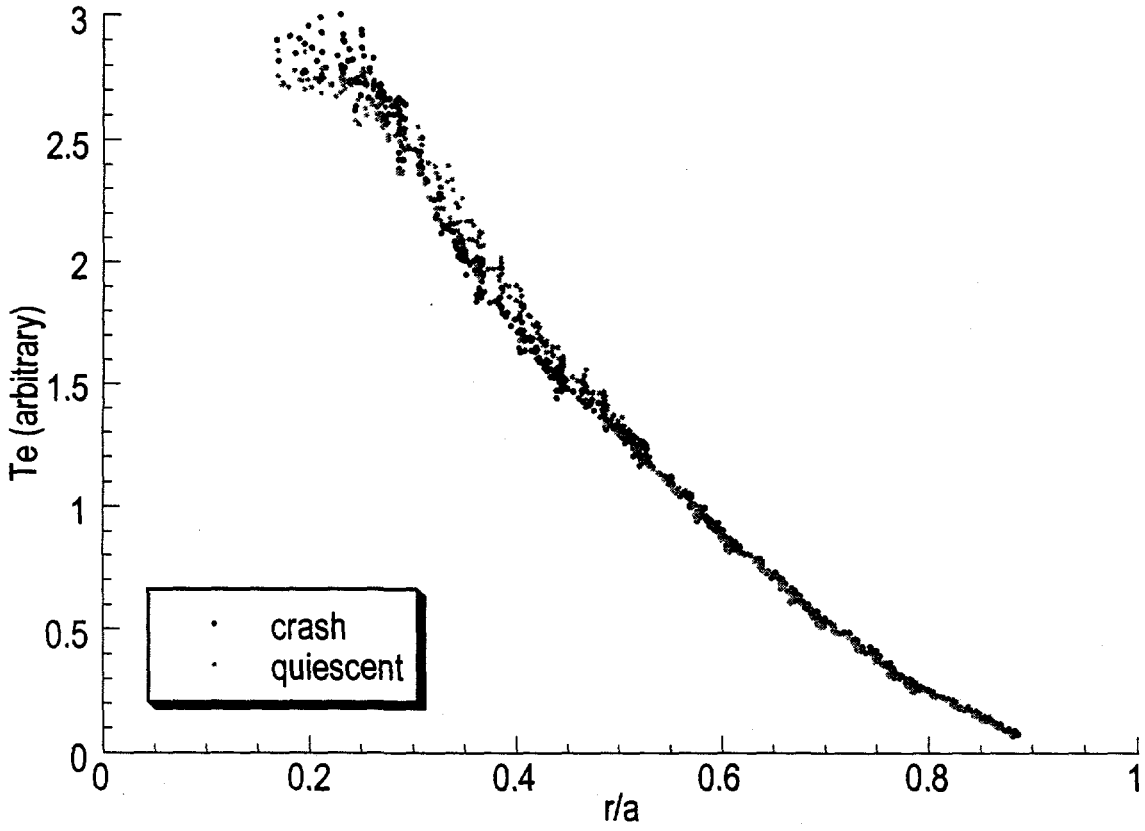

FIG. 1

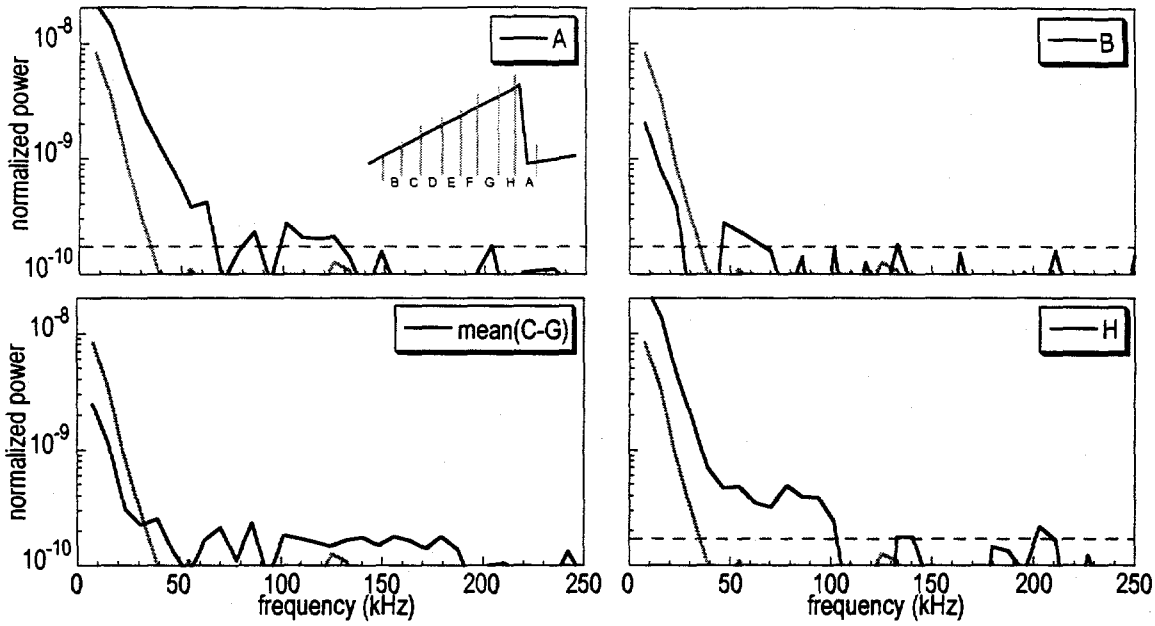
A
B
mean(C-G)
H
normalized power
10^{-8}
10^{-9}
10^{-10}
B C D E F G H A
0
50
100
150
200
250
frequency (kHz)

FIG. 2

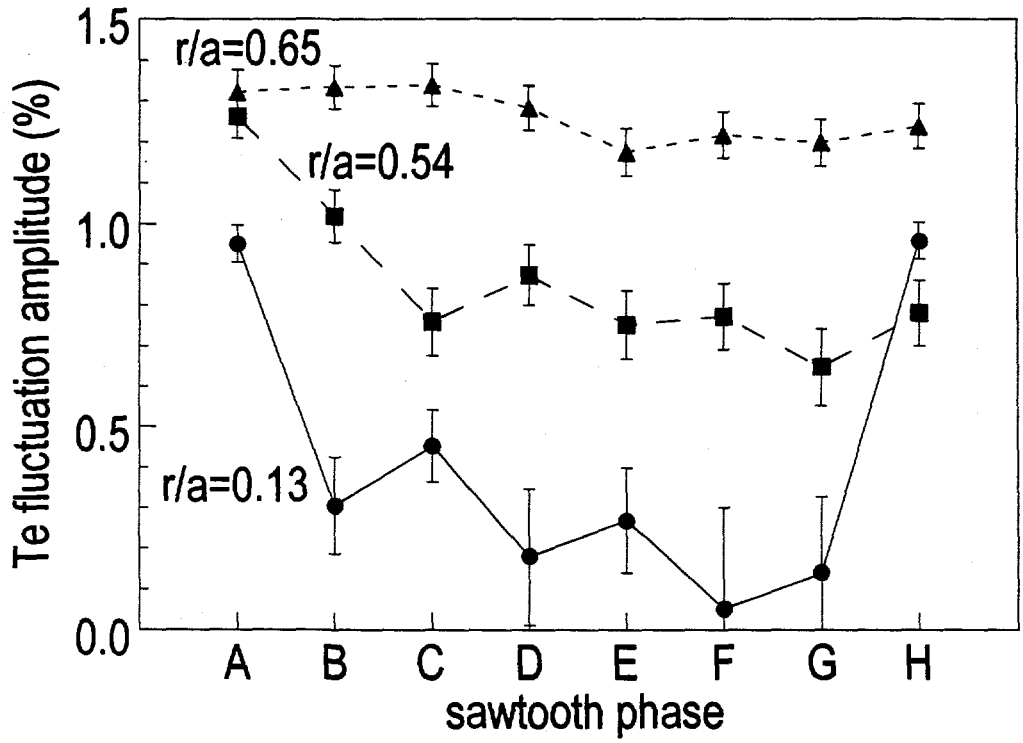
1.5
1.0
0.5
0.0
Te fluctuation amplitude (%)
r/a=0.65
r/a=0.54
r/a=0.13
A
B
C
D
E
F
G
H
sawtooth phase

FIG. 3

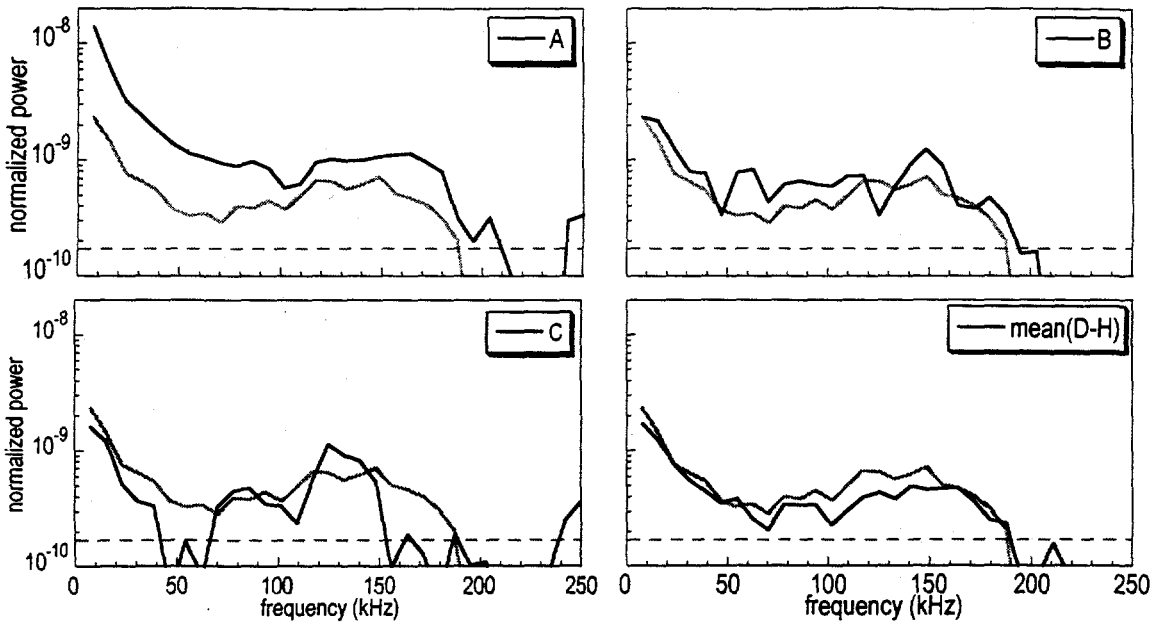
A
B
C
mean(D-H)
normalized power
10^{-8}
10^{-9}
10^{-10}
0
50
100
150
200
250
frequency (kHz)

FIG. 4

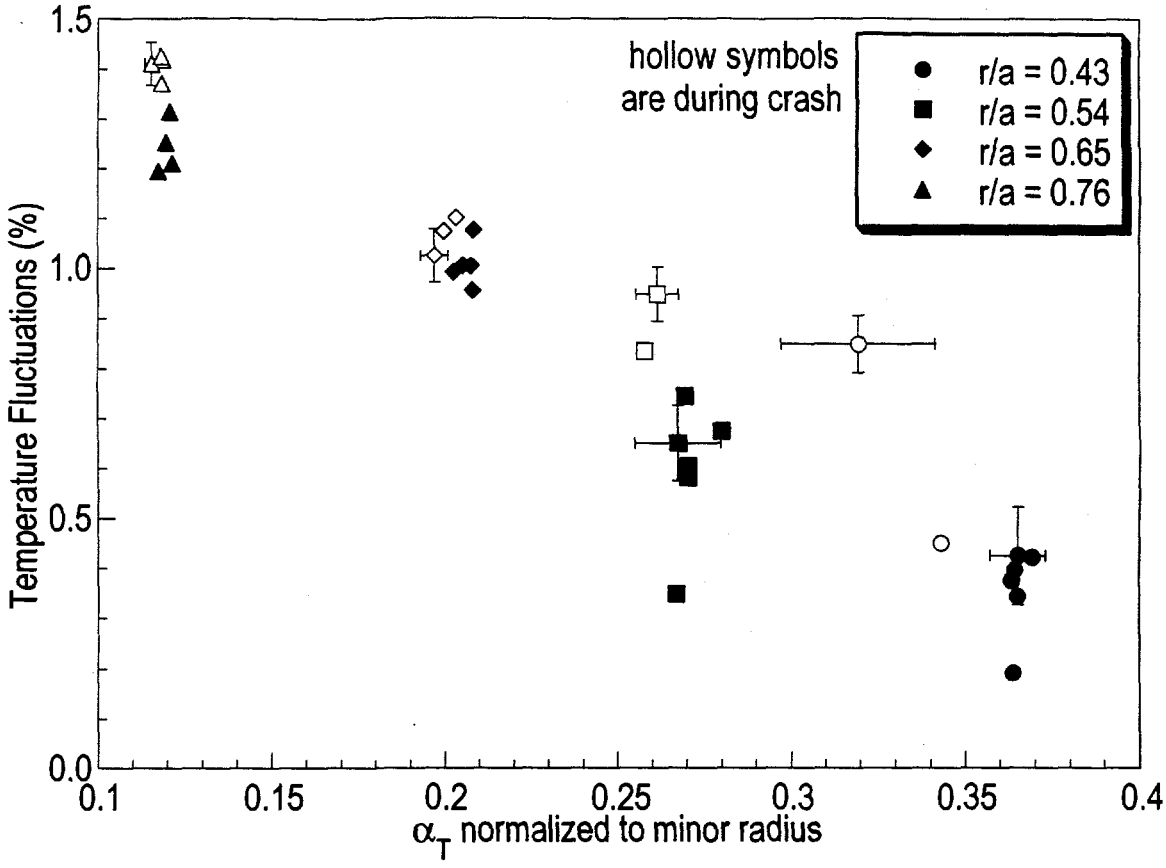
hollow symbols
are during crash
r/a = 0.43
r/a = 0.54
r/a = 0.65
r/a = 0.76
Temperature Fluctuations (%)
1.5
1.0
0.5
0.0
0.1
0.15
0.2
0.25
0.3
0.35
0.4
α_T normalized to minor radius

FIG. 5